

# Journal of Biomedical Optics

[SPIEDigitalLibrary.org/jbo](http://SPIEDigitalLibrary.org/jbo)

## **Raman spectroscopy for clinical-level detection of heparin in serum by partial least-squares analysis**

Ali Momenpour T. Monfared  
Vidhu S. Tiwari  
Markandey M. Tripathi  
Hanan Anis

# Raman spectroscopy for clinical-level detection of heparin in serum by partial least-squares analysis

Ali Momenpour T. Monfared,<sup>a</sup> Vidhu S. Tiwari,<sup>a</sup> Markandey M. Tripathi,<sup>b</sup> and Hanan Anis<sup>a</sup>

<sup>a</sup>University of Ottawa, School of Electrical Engineering and Computer Science, 800 King Edward, Ottawa, Ontario K1N 6N5, Canada

<sup>b</sup>Mississippi State University, Institute for Clean Energy Technology, Starkville, Mississippi 39759

**Abstract.** Heparin is the most widely used anti-coagulant for the prevention of blood clots in patients undergoing certain types of surgeries including open heart surgeries and dialysis. The precise monitoring of heparin amount in patients' blood is crucial for reducing the morbidity and mortality in surgical environments. Based upon these considerations, we have used Raman spectroscopy in conjunction with partial least squares (PLS) analysis to measure heparin concentration at clinical level which is less than 10 United States Pharmacopeia (USP) in serum. The PLS calibration model was constructed from the Raman spectra of different concentrations of heparin in serum. It showed a high coefficient of determination ( $R^2 > 0.91$ ) between the spectral data and heparin level in serum along with a low root mean square error of prediction  $\sim 4$  USP/ml. It enabled the detection of extremely low concentrations of heparin in serum ( $\sim 8$  USP/ml) as desirable in clinical environment. The proposed optical method has the potential of being implemented as the point-of-care testing procedure during surgeries, where the interest is to rapidly monitor low concentrations of heparin in patient's blood. © 2013 Society of Photo-Optical Instrumentation Engineers (SPIE) [DOI: 10.1117/1.JBO.18.2.027010]

Keywords: Raman spectroscopy; heparin; serum; partial least squares.

Paper 12705R received Nov. 1, 2012; revised manuscript received Jan. 24, 2013; accepted for publication Jan. 25, 2013; published online Feb. 20, 2013.

## 1 Introduction

Heparin is a polysaccharide (complex sugar) and is considered as a clinically important blood anticoagulant. It is commonly administered in patient's blood while undergoing open heart surgeries and in kidney dialysis. Adequate heparin treatment significantly decreases morbidity and mortality. Unfortunately, heparin also causes hemorrhagic complications from over-anticoagulation or heparin-induced blood disorders. It is thus imperative for physicians to monitor the amount of heparin in the blood accurately and in a timely fashion.

The guidelines on heparin monitoring is an elaborate document that recommends heparin doses to be administered to patients in various surgeries and illustrates methods of heparin monitoring along with their merits/demerits.<sup>1-3</sup> Traditionally, monitoring of heparin is based on functional test of anticoagulation such as activated clotting time (ACT) or activated partial thromboplastin time (aPTT).<sup>4-9</sup> The ACT test measures the anticoagulation effects of heparin by determining the time for blood with heparin to clot when induced by activators. The target range for ACT values varies from one surgery to another. For example, it is in the range of 400 to 600 s for cardiopulmonary bypass surgery.<sup>10</sup> However, ACT test results are prolonged (upto 15 min) in cases of thrombocytopenia, thrombopathy and hemodilution, and therefore correlate poorly with actual heparin levels.<sup>11,12</sup> The aPTT test is a relatively more sensitive laboratory technique in comparison to ACT for monitoring unfractionated heparin, especially in situations where the patient has coagulation disorders. It measures the time (aPTT) in which the optical density of blood plasma reaches a certain threshold in presence

of activators. The normal aPTT is in the range of 24 to 37 s, which is less than ACT; however, the incubation time of activators ( $\sim 10$  min), followed by addition of reagents (prior to aPTT measurement), makes the whole process time-consuming and tedious.

The ACT or aPTT values poorly correlate with actual heparin level in blood which may result in severe health complications. Therefore, alternate methods for monitoring heparin therapy which indicate direct quantification of heparin amount in patient's blood are gaining considerable interest. Some of the existing protocols based on the heparin concentration monitoring are protamine sulphate titration, anti-Xa, etc.<sup>13-16</sup> However, protamine sulphate titration results in excess post operative bleeding or platelet activation if there is an overdose of protamine sulphate. The anti-Xa is exclusively performed to monitor low-molecular weight heparin. It measures the heparin content indirectly by measuring the artificial factor  $X$  which is inversely related to the heparin activity.<sup>16</sup> The limitation of anti-Xa is that it is an off-line method (laboratory technique) and involves various steps that make it very time-consuming.

Each of the above mentioned techniques, based on either testing the anticoagulation effect or detecting the heparin concentration, have their own advantages and disadvantages. The approximate detection time and accuracy of these techniques are summarized in Table 1. An ideal technique, for use in heparin therapy, must be instantaneous, accurate, simple, and minimally affected by patients' physical condition or medical history.

Based upon these considerations, we have implemented Raman spectroscopy in conjunction with partial least-squares (PLS) analysis, an important multivariate analysis tool, for measuring the heparin concentration in serum at a clinical

Address all correspondence to: Vidhu S. Tiwari, University of Ottawa, School of Electrical Engineering and Computer Science, 800 King Edward, Ottawa, Ontario K1N 6N5, Canada. Tel: +1 613 562 5800 Ext: 2502; Fax: 613 562 5664; E-mail: vidhu2u@gmail.com

**Table 1** Different techniques of laboratory monitoring heparin.

Method	Detection time (min)	Estimated detection accuracy (USP/ml)
ACT	~7 to 15	0.1
aPTT	~10	0.1
Anti-Xa	~60	0.01
Protamine sulfate titration	~5	0.1

level. The Raman scattered light occurs at frequencies that are shifted from the incident laser light by the changes in vibrational energies of molecule. By measuring the frequency and intensity of inelastically scattered light from the sample, the molecular composition of the sample can be measured qualitatively as well as quantitatively.<sup>17</sup> Raman signal is usually weak because only one photon out of  $10^8$  is Raman scattered. PLS analysis is useful in quantitative analysis especially when the Raman signal is weak or when there is an overlap of Raman bands of interest with that of sampling media (e.g., serum, blood, etc). In such situations, PLS analysis can aid in the identification, of the spectral regions, for inferring the sample quantity as it scans the entire Raman spectrum or the spectral segments that contain Raman bands of interest.<sup>18–24</sup>

The past decade has seen many reports on applying Raman spectroscopy in the medical arena using multivariate analysis (MVA).<sup>25–29</sup> In this context, one body of work is dedicated toward diagnosing various types of cancers on the basis of identifying a spectral contrast between healthy and malignant cells/tissues.<sup>25,26</sup> Another kind of work is focused on identifying and screening clinically important molecules, such as glucose, creatinine, urea, and lactic acid, in various kinds of bodily fluids/matrix including serum, urine, aqueous humor, and many more.<sup>27–29</sup> It is more evident in the light of solute-solvent problem, which is also the subject matter of our work.

The present study aims to monitor the concentration of heparin, in blood derived serum, by Raman spectroscopy with PLS analysis. It offers a novel alternative to measure the heparin content in comparison to the previously described laboratory methods including fluorescence, surface plasmon resonance, field effect transistor, and membrane-based ion-selective electrodes.<sup>30–32</sup> These methods involve indirect detection by using heparin probes such as protamine or synthetic cationic polymers. Moreover, they are complicated and based on either surface affinity capture or an automated heparin protamine titration which limits the system sensitivity for detecting lower concentrations of heparin in blood. Also, accuracy of such methods depends on the cross reaction of heparin with the labeling agent which may give false results. In the past, Khetani et al. detected heparin quantity by enhancing its Raman signal by mediating a strong light-sample interaction within the hollow core photonic crystal fiber (HC-PCF).<sup>33</sup> However, in Khetani et al.'s work, maintaining an identical light coupling condition from one sample filled HC-PCF to another was challenging. Hence, we used Raman (i.e., sample in cuvette) rather than enhanced Raman (i.e., sample in hollow core fiber as in Khetani et al.'s paper) and prepared a large number of spectral data sets for multivariate analysis. Our proposed method is simple and directly measures heparin concentration up to the

clinical level. In most surgeries, clinical level or the physiological level of heparin is considered as less than 10 United States Pharmacopeia (USP) of heparin per milliliter of the patient's blood. Our method is faster in comparison to the traditional methods of heparin-monitoring as the time required for spectral data acquisition and feeding it to the prebuilt MVA model is around 1 min. The accuracy of the PLS model has been tested by predicting the heparin concentration in the sample set that was not involved in its construction.

The paper is organized in the following manner. We begin with sample preparation followed by describing the experimental setup. In subsequent sections, we present the quantification procedure for detecting heparin by PLS regression model. Finally, we compare the predicted heparin concentration with the measured heparin concentration in the sample set which was not used in the construction of the PLS model.

## 2 Experimental

### 2.1 Sample Preparation

Blood samples were obtained from a local bovine slaughter house. Serum was prepared by centrifuging the blood at a speed of 4000 rpm for 20 min. The clinical-grade heparin samples were purchased from Pharmaceutical Partners of Canada (PPC Inc.). The sample solutions were prepared by adding different amounts of heparin, in the range of 2 to 25  $\mu\text{L}$ , to a fixed volume (3 mL) of serum. In order to prepare the first set of serum-heparin sample mixtures, we equally divided the serum of the first cow into 10 parts, each with a volume of 3 mL. We then added 2.5  $\mu\text{L}$  of heparin to the first sample of first cow and 5  $\mu\text{L}$  of heparin to the second sample of first cow and so on. The same procedure was repeated for the second cow. For the other three cows, the sample preparation was started by adding 2  $\mu\text{L}$  of heparin to 3 mL of serum with the same interval (2.5  $\mu\text{L}$ ). Overall, there were a total of 50 samples ( $5 \times 10$ ). The concentration of heparin in serum was labelled in terms of USP per mL of serum in accordance with the terminology used in the clinical environment. The USP describes the potency of the drug in clinical applications. The heparin concentrations in 50 different serum-heparin samples from 5 different cow's blood are shown in Table 2. It is to be noted that 1  $\mu\text{L}$  of heparin had a potency of 10 USP (0.094 mg). Hence, the heparin concentration/potency (in terms of its USP values in 1 mL of serum) was calculated from the actual volume of heparin which was added to 3 mL of serum as shown in Table 2.

### 2.2 Experimental Configuration

Figure 1 shows the schematic of experimental setup. The experimental configuration involved a 785-nm continuous wavelength multimode laser (B&W Tek Inc.) with a maximum output power of 450 mW. The laser beam was first collimated by a plano-convex lens (L1) and passed through a bandpass filter (BP), centered at 785 nm ( $\pm 2$  nm), to filter out other wavelength components around 785 nm from the laser. Then, it was directed through a dichroic filter (R785RDC, Chroma Technologies Corp.) which reflected 785 nm ( $\pm 5$  nm) at an angle of 45 deg and transmitted light in the 790 to 1000 nm range. The dichroic filter acted as a reflector for the laser beam which was further focused onto the sample in quartz-cuvette by a 10 $\times$  microscopic objective lens (L2, CVI Melles Griot/04

**Table 2** The heparin concentration in serum for 50 sets of sample mixtures.

Sample set #1		Sample set #2		Sample set #3		Sample set #4		Sample set #5	
Serum-heparin no.	Concentration (USP/ml)								
SH-1	8.3	SH-11	8.3	SH-21	6.6	SH-31	6.6	SH-41	6.6
SH-2	16.6	SH-12	16.6	SH-22	15	SH-32	15	SH-42	15
SH-3	25	SH-13	25	SH-23	23.3	SH-33	23.3	SH-43	23.3
SH-4	33.3	SH-14	33.3	SH-24	31.6	SH-34	31.6	SH-44	31.6
SH-5	41.6	SH-15	41.6	SH-25	40	SH-35	40	SH-45	40
SH-6	50	SH-16	50	SH-26	48.3	SH-36	48.3	SH-46	48.3
SH-7	58.3	SH-17	58.3	SH-27	56.6	SH-37	56.6	SH-47	56.6
SH-8	66.6	SH-18	66.6	SH-28	65	SH-38	65	SH-48	65
SH-9	75	SH-19	75	SH-29	73.3	SH-39	73.3	SH-49	73.3
SH-10	83.3	SH-20	83.3	SH-30	81.6	SH-40	81.6	SH-50	81.6

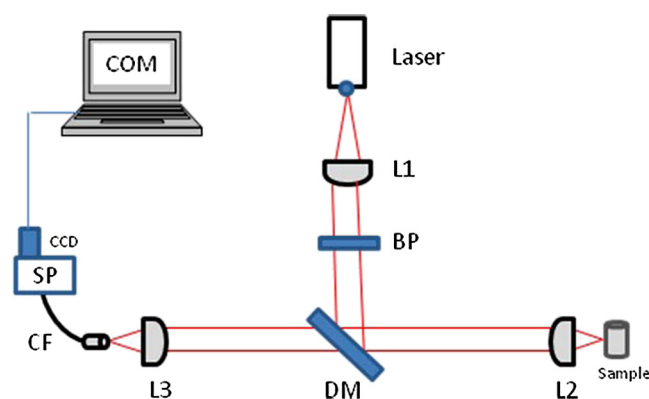


**Fig. 1** Schematic of the setup. L1, collimating lens; BP, band pass filter; DM, dichroic mirror; L2, microscope objective lens for focusing light onto the sample; L3, microscope objective lens for backward light collection; CF, collection fiber; SP, spectrograph; CCD, CCD camera; COM: computer.

OAS 010) with numerical aperture (N.A.) as  $\sim 0.25$ . Furthermore, the dichroic filter also acted as a high-pass filter for the light scattered backward from the sample, thus, allowing only the Raman wavelengths to pass through. The filtered Raman light was then imaged onto a fiber bundle (Fiberoptic System Inc., 30 multimode fiber, N.A. = 0.22) by another  $6.3\times$  microscopic objective lens (L3) with N.A. as  $\sim 0.20$ . The diameters of core and cladding were 100 and 125 microns, respectively. The fiber bundle consisted of 30 identical fibers with a packing efficiency of 80%. The output of the fiber bundle was interfaced into a Kaiser  $f/18i$  Spectrograph with a thermoelectrically cooled Andor charge-coupled device camera. The spectral resolution of the spectrometer was  $2.05\text{ cm}^{-1}$ . Andor SOLIS software was used for spectral data acquisition and spectra were monitored on the data acquisition computer. The laser beam power at sample was 250 mW and the acquisition time for recording a spectrum was 24 s. The self-configured optical

configuration, as described above, was well optimized for achieving Raman signal of heparin with high signal-to-noise ratio.

### 2.3 Multivariate Data Analysis

The serum contains several biological components including albumin, glycoproteins, immunoglobulins, and lipoproteins that give rise to the strong spectral (fluorescence) background. The weak Raman signal of heparin was completely swamped in the presence of spectral background of serum. Consequently, no direct correlation between the heparin concentration and its Raman bands could be ascertained. This problem became further exacerbated while detecting heparin at the physiological level, in which case the concentration of heparin was below 10 USP/mL. Under these circumstances, Raman spectral data sets, for serum-heparin mixtures, were used to construct a calibration model for performing the PLS analysis by Unscrambler® X version 10.0 (CAMO, Corvallis, OR). The PLS models were constructed from the spectral and analytical data. The PLS regression is relevant for a two-dimensional ( $X$ ,  $Y$  variable) data set where the response  $Y$ -variable (analytical data) depends on more than one explanatory  $X$ -variable (spectral wavelength).<sup>19,34</sup> Prior to PLS regression, the spectra were background subtracted by Unscrambler® software to remove the fluorescence effect. Also, Raman spectral data were normalized using multiple scattering correction (MSC) to correct the variability of baseline data. Such variations are caused by scattering or other physical phenomena.

The calibration model was validated by test set validation (TSV) where the spectral data corresponding to four cows (200 spectra), also referred as training set/modeling group, were selected to construct the PLS model. The remaining one cow spectral data (50 spectra), also referred as test group, was used to validate the constructed model. The details of TSV procedure are further discussed in Sec. 3.3. The construction of an efficient PLS model involved careful selection of a number of

principal components (PCs). The PLS model was evaluated against various statistical parameters including root mean square error of calibration (RMSEC), root mean square error of prediction (RMSEP), and coefficient of determination ( $R^2$ ). The optimum number of PCs was used in the calibration model.

### 3 Results and Discussion

#### 3.1 Raman Spectral Data

The present study was primarily focused on quantitative measurement of heparin in sample mixtures of heparin and serum. Fifty samples of heparin-serum mixtures, with different compositions of heparin (within the range of ~6 to 83 USP/mL), were prepared. These were named as SH1, SH2, ..., SH50 as shown in Table 2. The Raman spectrum of pure clinical grade heparin is shown in Fig. 2. The assignment of Raman bands of heparin has already been reported by Atha et al.<sup>35</sup> The overlapped Raman bands, due to the symmetric  $\text{SO}_3$  vibration, were located at  $\sim 1035 \text{ cm}^{-1}$  (N- $\text{SO}_3$  vibration),  $1045 \text{ cm}^{-1}$  (6-O- $\text{SO}_3$  vibration), and  $1060 \text{ cm}^{-1}$  (3-O- $\text{SO}_3$  vibration). The two medium intensity peaks of heparin, around  $827$  and  $893 \text{ cm}^{-1}$ , have been assigned to the C-H deformation of  $R$  and  $\alpha$  and  $\beta$  anomers of the 2-acetamido-2-deoxy-D-glucose residues along with the presence of low-intensity peak  $\sim 1000 \text{ cm}^{-1}$  (C-N stretching).<sup>35</sup> The spectral range of  $600$  to  $1500 \text{ cm}^{-1}$  was used for the quantitative analysis of heparin as it contained the prominent Raman peaks of heparin. However, Raman spectrum of serum-heparin mixture barely exhibited any of the Raman peaks of heparin when the concentration of heparin was extremely low. This fact is evident in Fig. 2 which shows how the strong fluorescence background of serum completely obscured the weak Raman signal of heparin. Figure 2 also indicates a fall in the fluorescence background of serum with the consecutive increase of heparin concentration. Moreover, serum has various intrinsic chemicals that give rise to Raman peaks which interferes with the Raman peak of heparin.<sup>22</sup> Consequently, correlating the Raman bands of heparin with its concentration became practically impossible by merely formulating a simple calibration model. Hence, PLS models were constructed based on Raman spectra of serum and heparin mixtures.

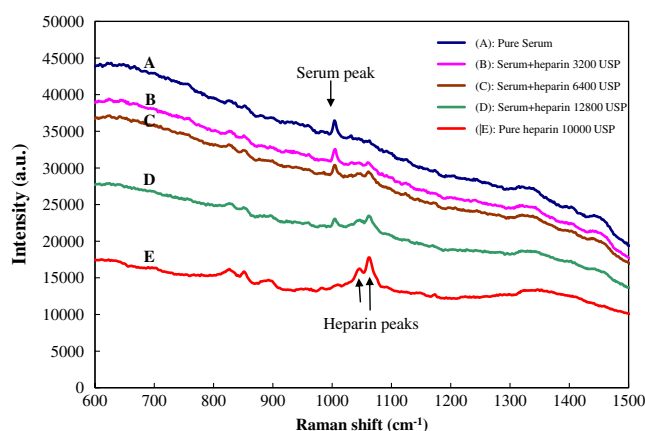


**Fig. 2** Raman spectrum of pure serum, pure heparin, and mixtures of heparin and serum.

#### 3.2 Loading and Score Plots

Loading plots can be seen as the bridge between variable space and the principal component space which also provides a projection view of the inter-variable relationship. In simple terms, they indicate the individual contribution of each variable (wavenumbers in our case) toward each PC.<sup>19</sup> The loadings of the first and second PC are shown in Fig. 3(a). The prominent Raman bands around  $1040$  to  $1070 \text{ cm}^{-1}$ , corresponding to symmetric  $\text{SO}_3$  vibration, are represented in PC1. It constitutes the part of “systematic variation” in the overall spectral range which also forms the structure of the regression model. Another point of observation is the dip around  $1000 \text{ cm}^{-1}$  in PC1. It is due to the decrease in the Raman peak of serum around  $1000 \text{ cm}^{-1}$  (Phenylalanine, C-C stretching) while the heparin amount was changed with respect to serum.<sup>22</sup> The broad band, in the wavenumber range of  $1300$  to  $1450 \text{ cm}^{-1}$ , in PC1 may be due to spectral background of silica. On the other hand, PC2 shows variation of serum peak  $\sim 1000 \text{ cm}^{-1}$ . The remaining part of PC2 describes the “unexplained” component of the model which can be ascribed to “random noise.”

On the other hand, the regression coefficients plot, Fig. 3(b), explains the most important variables (wavenumbers) in the PLS model. This figure shows that wavenumbers around  $1000$ ,  $1035$ , and  $1045 \text{ cm}^{-1}$  were used for the quantitative analysis in this model. Similar to loading vectors, score vectors can be plotted against each other. These plots are complementary in nature and provide significant information about the object and the variables when studied together.<sup>19</sup> Moreover, score plots indicate any

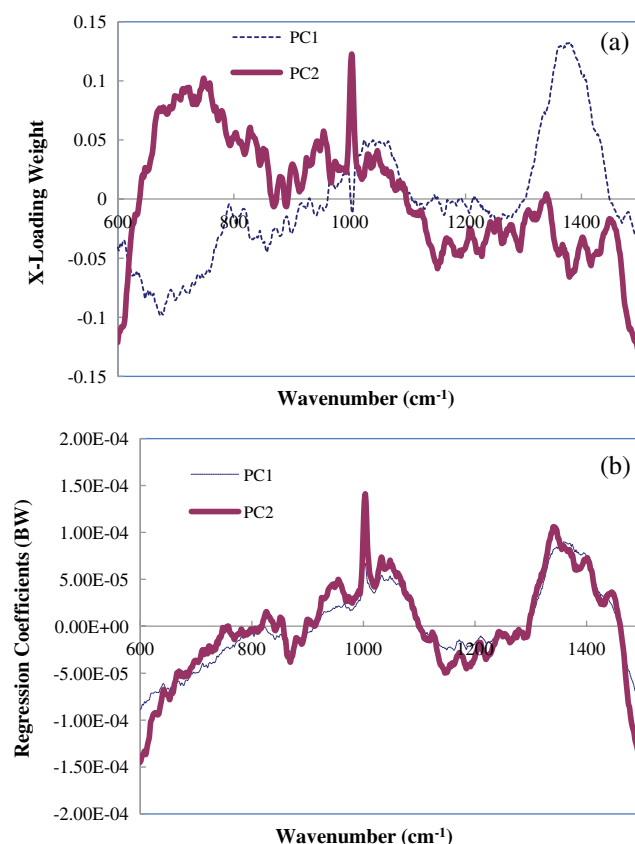


**Fig. 3** (a) Loadings of the first and second principal component of the MSC-corrected spectrum in the range of  $600$  to  $1500 \text{ cm}^{-1}$ . (b) Regression coefficients of PLS model for PC1 and PC2.

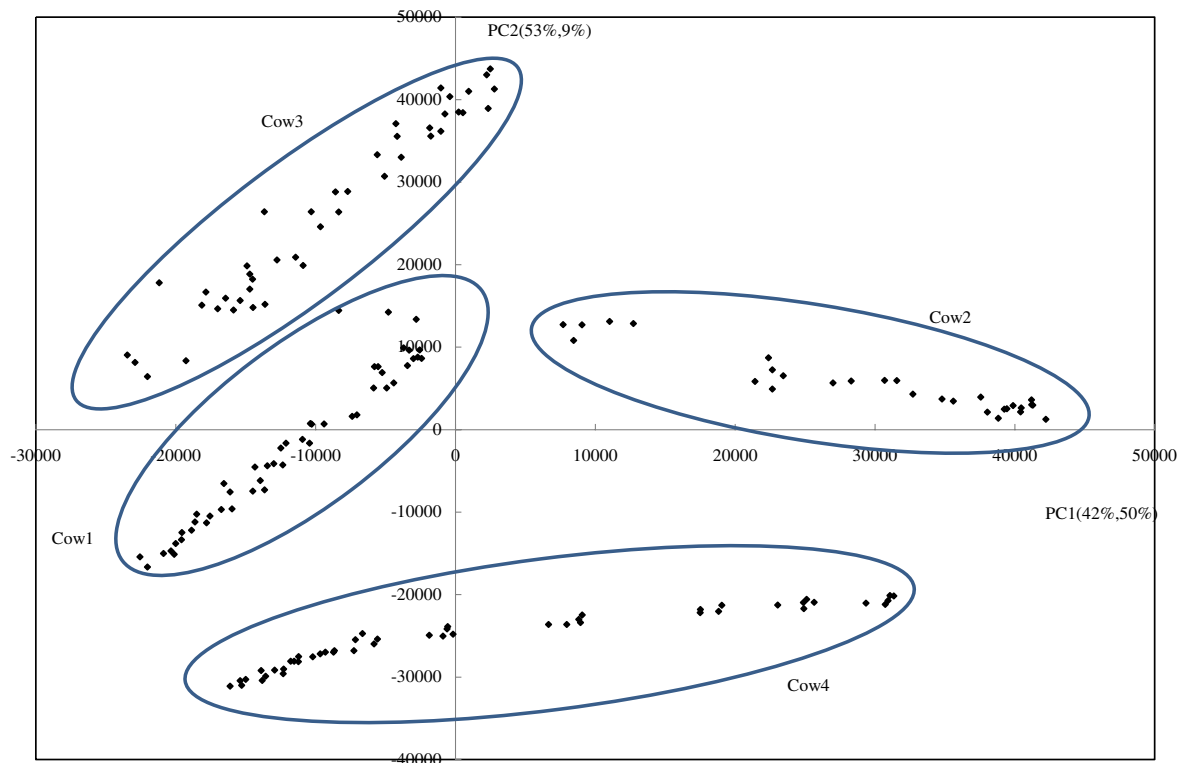


**Fig. 4** Score plot for first and second principal component of the MSC-corrected spectrum in the range of 600 to 1500  $\text{cm}^{-1}$ .

clustering of variables or presence of outliers to be eliminated. The score plot of PC1 and PC2 is shown in Fig. 4. The first two PCs indicate that 95% (X1 42%, X2 53%) of the X variance, explains 59% (Y1 50%, Y2 9%) of response heparin level. This figure shows very distinguishable clusters in the samples which means most of the samples in each cluster are similar. Loading and score plots have significant relevance in this work. It is mainly due to an overlap between Raman band(s) of heparin (solute) with that of serum (solvent), in which case the spectrum does not indicate an explicit correlation of heparin band intensity with the low heparin concentration. Loading plot, in particular, accounts for the variation of regression coefficients and presents the actual contribution of heparin in the overlapped Raman bands of heparin and serum.

### 3.3 PLS Model

The Raman spectra of 50 samples of serum and heparin were recorded. For each sample, five Raman spectra were collected to ensure consistency in the replicated measurements. Hence, the total number of Raman spectra was 250. The PLS models were developed by using the data sets of four cows for constructing the model and a data set of one cow for independent prediction. For example, Model #1 was developed by using the data sets of second, third, fourth, and fifth cow, Model #2 was developed by using the data sets of first, third, fourth, and fifth cow, and so on. A few sample outliers were identified by the Unscrambler® software and removed accordingly from the analysis. Table 3 shows the result of the five possible models,  $R^2$ , RMSEC, and RMSEP of each model, with and without MSC, for the spectral range of 600 to 1500  $\text{cm}^{-1}$ . This table indicates that MSC has reduced the RMSEP values in all models. These PLS models were validated based on TSV method.

**Table 3** PLS models of heparin concentrations in serum with TSV.

No.	Preprocessing	Test set validation			
		$R^2$ Cal	RMSEC	RMSEP	PCs
1	No MSC	0.86	8.74	4.11	3
	MSC	0.91	6.79	2.73	3
2	No MSC	0.90	7.38	9.83	4
	MSC	0.94	5.03	3.82	4
3	No MSC	0.93	6.12	8.75	5
	MSC	0.98	3.20	5.01	5
4	No MSC	0.93	6.28	10.7	5
	MSC	0.97	3.67	4.23	5
5	No MSC	0.93	5.87	6.56	6
	MSC	0.98	2.41	4.19	6

It has been established that TSV gives lower prediction error compared to full cross validation (FCV) in situations where the sample set is large enough, which is similar to our case.<sup>19</sup>

The PLS model, as obtained from preprocessed data, involved three to six PCs. The optimal number of PCs was ascertained by looking at Y-variable residuals versus PC numbers (not shown here) and determining the values of PCs where the residual variance tends to zero. The numbers of PCs in each of the five different PLS models were optimized to reduce

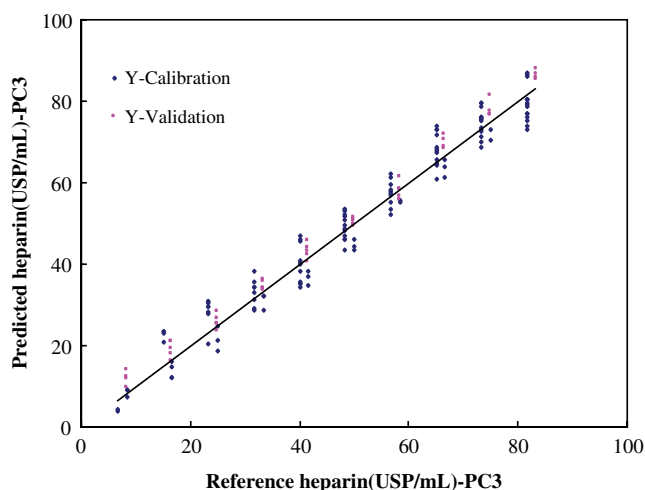


**Fig. 5** PLS regression model for predicting heparin content in serum in 600 to 1500  $\text{cm}^{-1}$  spectral range using multiple scattering correction and test set validation.

RMSEP values as indicated in Table 3. Due to some variation in blood samples from one cow to another, it was expected that selected number of PCs would vary from one model to other where the key consideration was to establish higher degree of prediction accuracy. All of the five PLS models with MSC preprocessing show high  $R^2$  (more than 0.91) and low RMSEP (less than 5 USP/mL). Table 3 indicates an average of RMSEP values for all the five PLS models with MSC preprocessing,  $\sim 4$  USP/mL, with less fluctuation from one model to another (standard deviation  $\sim 0.82$ ). Thus, it is clear that the RMSEP values were quite consistent from one model to another which indicates a consistency in the prediction accuracy of all the five constructed PLS models for measuring heparin concentration in serum.

The prediction result of one of the PLS models is shown in Fig. 5. This calibration curve indicates the measured and predicted value of heparin in serum. This model was based on preprocessed data (with MSC) and validated with TSV method. According to this calibration curve, the RMSEP error in TSV (within the range of 6 to 84 USP/mL) is about 2.73 USP/mL, which corresponds to  $\sim 3.2\%$ . The overall conclusion is that extremely low amounts of heparin, as low as  $\sim 8$  USP, can be detected with high accuracy as desired in a clinical environment.

### 3.4 Unknown Sample Prediction

The guideline of heparin administration is complex and depends on the patient's medical condition and other physical attributes (age, weight, etc). A reliable and accurate method of heparin monitoring must provide a consistent result when the different dose of heparin is given to one patient. With this consideration, next phase of investigation focused on predicting the heparin concentrations in those samples (unknown samples) which were not involved in the construction of model. It is also referred to as external validation, where the sample data set is divided into "training set" and "validation set." A comprehensive model was constructed which involved blood samples of four different cows (training set). The model was then externally validated against the sample data (validation set) which was kept aside during its construction. It predicted a different amount of heparin in single serum sample, in the range of 8.3 to

**Table 4** The prediction of different heparin concentrations in serum for one unknown sample.

Measured heparin (USP/ml)	Predicted heparin (USP/ml)	Deviation (USP/ml)
8.3	9.7	2.2
16.6	15.8	2.3
25	25.3	2.3
33.3	33.6	2.4
41.6	40.6	2.6
50	50.2	2.7
58.3	58.3	2.8
66.6	68.6	3.1
75	76.4	3.2
83.3	86.4	3.1

83.3 USP/mL. These results are summarized in Table 4 which shows that the PLS model can reliably predict different concentrations of heparin with deviation in the range of  $\sim 2.2$  to 3.2 USP/mL. The deviation is a function of the RMSEP of the model and confirms that the constructed model has good prediction ability for different concentrations of heparin in a single (unknown) sample.

We have demonstrated an alternative method of heparin detection which is based on Raman spectroscopy and PLS analysis. To make it further useful for rapid monitoring of heparin in a surgical environment, the process of spectral data acquisition, and subsequent feeding into the prebuilt calibrated model, could be fully automated. Also, the time spent centrifuging the blood in this study can be further shortened. It can be achieved by subjecting the whole blood to a "composite media" filter. Under this situation, the serum sample can be obtained within a few seconds instead of using a centrifuge which takes 15 to 20 min to separate serum from blood.

## 4 Conclusions

The present work illustrates a simple procedure for monitoring heparin concentration in serum by applying partial least squares on the Raman spectral data of heparin and serum mixtures. Five different PLS regression models were constructed from the sample data with high coefficients of determination ( $R^2$ ) and lower values of RMSEP. The RMSEP values were found to be in the range of 2 to 5 USP/mL, with an average of  $\sim 4$  USP/mL, and standard deviation of  $\sim 0.8$ . This indicates a consistency in the prediction accuracy of various PLS models (based on different sets of sample data) for measuring different concentrations of heparin. Our results indicate that PLS regression model can determine heparin concentration as low as  $\sim 8$  USP/mL as desired in a clinical environment. In summary, Raman spectroscopy and PLS not only measures heparin quantitatively, but also provides reliable estimates of heparin concentrations irrespective of variability in serum samples. Future work will focus on determining the heparin concentration directly from whole blood.

## Acknowledgments

This work was supported by Ontario Centres of Excellence and The Technology Transfer and Business Enterprise at the University of Ottawa. The authors would like to acknowledge the support of Animal Care and Veterinary Service. We would also like to thank Gurinder Gill from Heart Institute and Louis Tremblay from Department of Chemical Engineering from University of Ottawa.

## References

1. T. Baglin et al., "Guidelines on the use and monitoring of heparin," *Br. J. Haematol.* **133**(1), 19–34 (2006).
2. J. D. Olson et al., "Laboratory monitoring of unfractionated heparin therapy," *Arch. Pathol. Lab. Med.* **122**(9), 782–798 (1998).
3. J. H. Joist et al., *Point-of-Care Monitoring of Anticoagulation Therapy: Approved Guideline*, NCCLS, Pennsylvania (2004).
4. P. D. Raymond et al., "Heparin monitoring during cardiac surgery. Part 2: calculating the overestimation of heparin by the activated clotting time," *Perfusion* **18**(5), 277–281 (2003).
5. E. K. Heres et al., "The clinical onset of heparin is rapid," *Anesth. Analg.* **92**(6), 1391–1395 (2001).
6. S. Kitchen et al., "Wide variability in the sensitivity of APTT reagents for monitoring of heparin dosage," *J. Clin. Pathol.* **49**(1), 10–14 (1996).
7. S. A. Spinler et al., "Point of care anticoagulation monitoring. Part 2: unfractionated heparin and low molecular weight heparin," *Ann. Pharmacother.* **39**(7), 1275–1285 (2005).
8. Y. Nosé, "Hemodialysis patients' deaths in the USA by contaminant suspected heparin originating from China," *Artif. Organs* **32**(6), 425–426 (2008).
9. D. Perry and T. Todd, "Activated partial thromboplastin time [APTT]," <http://www.practical-haemostasis.com/Screening%20Tests/aptt.html> (29 July 2012).
10. J. A. Young, C. T. Kisker, and D. B. Doty, "Adequate anticoagulation during cardiopulmonary bypass determined by activated clotting time and the appearance of fibrin monomer," *Annals Thorac. Surg.* **26**(3), 231–240 (1978).
11. P. D. Raymond et al., "Heparin monitoring during cardiac surgery. Part 1: validation of whole-blood heparin concentration and activated clotting time," *Perfusion* **18**(5), 269–276 (2003).
12. T. Ammar et al., "The effects of thrombocytopenia on the activated coagulation time," *Anesth. Analg.* **83**(6), 1185–1188 (1996).
13. R. T. Hall et al., "Protamine sulfate titration for heparin activity in neonates with indwelling umbilical catheters," *J. Pediatr.* **88**(3), 467–472 (1976).
14. M. A. Smythe, J. C. Mattson, and J. M. Koerber, "The heparin anti-Xa therapeutic range," *Chest* **121**(1), 303–304 (2002).
15. O. Shigetani et al., "Low-dose protamine based on heparin-protamine titration method reduces platelet dysfunction after cardiopulmonary bypass," *J. Thorac. Cardiovasc. Surg.* **118**(2), 354–360 (1999).
16. I. Weinberg, "Anti Xa," <http://www.angiologist.com/anti-xa> (2 June 2011).
17. M. J. Pelletier, *Analytical Applications of Raman Spectroscopy*, Blackwell Science, Malden (1999).
18. M. J. Pelletier, "Quantitative analysis using Raman spectroscopy," *Appl. Spectrosc.* **57**(1), 20A–42A (2003).
19. K. H. Esbensen, *An Introduction to Multivariate Data Analysis and Experimental Design*, 5th ed., Camo Inc., Oslo, Norway (2004).
20. C. M. McGoverin et al., "Raman spectroscopic quantification of milk powder constituents," *Anal. Chim. Acta* **673**(1), 26–32 (2010).
21. R. M. El-Abassy et al., "Fast determination of milk fat content using Raman spectroscopy," *Vib. Spectrosc.* **56**(1), 3–8 (2011).
22. C. A. Drumm and M. D. Morris, "Microscopic Raman line-imaging with principal component analysis," *Appl. Spectrosc.* **49**(9), 1331–1337 (1995).
23. P. Matousek, "Subsurface probing in diffusely scattering media using spatially offset Raman spectroscopy," *Appl. Spectrosc.* **59**(4), 393–400 (2005).
24. G. V. Nogueira et al., "Raman spectroscopy study of atherosclerosis in human carotid artery," *J. Biomed. Opt.* **10**(3), 031117 (2005).
25. S. Feng et al., "Nasopharyngeal cancer detection based on blood plasma surface-enhanced Raman spectroscopy and multivariate analysis," *Biosens. Bioelectron.* **25**(11), 2414–2419 (2010).
26. J. L. Pichardo-Molina et al., "Raman spectroscopy and multivariate analysis of serum samples from breast cancer patients," *Laser Med. Sci.* **22**(4), 229–236 (2007).
27. M. Ren and M. A. Arnold, "Comparison of multivariate calibration model for glucose, urea, and lactate from near-infrared and Raman spectra," *Anal. Bioanal. Chem.* **387**(3), 879–888 (2007).
28. J. W. McMurdy and A. J. Berger, "Raman spectroscopy-based creatinine measurement in urine samples from multipatient population," *Appl. Spectrosc.* **57**(5), 522–525 (2003).
29. D. Qi and A. J. Berger, "Chemical concentration measurement in blood serum and urine samples using liquid-core optical fiber Raman spectroscopy," *Appl. Opt.* **46**(10), 1726–1734 (2007).
30. H. Szelke, J. Harenberg, and R. Krämer, "Detection and neutralisation of heparin by fluorescent ruthenium compound," *Thromb. Haemost.* **102**(5), 859–864 (2009).
31. K. Gaus and E. Hall, "Evaluation of surface plasmon resonance (SPR) for heparin assay," *J. Colloid Interface Sci.* **194**(2), 364–372 (1997).
32. N. Milovic et al., "Monitoring of heparin and its low-molecular-weight analogs by silicon field effect," *Proc. National Acad. Sci. U. S. A.* **103**(36), 13374–13379 (2006).
33. A. Khetani et al., "Monitoring of heparin concentration in serum by Raman spectroscopy within hollow core photonic crystal fiber," *Opt. Express* **19**(16), 15244–15254 (2011).
34. M. Tripathi et al., "Reflection-absorption-based near infrared spectroscopy for predicting water content in bio-oil," *Sens. Actuators B* **136**(1), 20–25 (2009).
35. D. H. Atha, A. K. Gaigalas, and V. Reipa, "Structural analysis of heparin by Raman spectroscopy," *J. Pharm. Sci.* **85**(1), 52–56 (1996).